

Nonmagnetic impurity resonance states as a test of superconducting pairing symmetry in CeCoIn₅

Bin Liu*

Department of Physics, Beijing Jiaotong University, Beijing 100044, China

(Received 17 May 2013; published 20 December 2013)

We theoretically study the effect of a nonmagnetic impurity in heavy fermion superconductor CeCoIn₅ within a coherent three-dimensional Anderson lattice model and the T -matrix approximation approach. By considering two known possible pairing symmetry candidates $d_{x^2-y^2}$ and d_{xy} , we find that although both total density of states exhibit a similar V-shaped gaplike feature, only $d_{x^2-y^2}$ -wave pairing symmetry gives rise to robust intragap impurity resonance states reflected by the resonance peaks near the Fermi energy in the local density of states. These features can be readily probed by scanning tunneling microscopy experiments, and are proposed to shed light on the pairing symmetry and provide hints on the microscopic mechanism of unconventional superconductivity in the Ce-based heavy fermion superconductors.

DOI: [10.1103/PhysRevB.88.245127](https://doi.org/10.1103/PhysRevB.88.245127)

PACS number(s): 74.25.Jb, 74.20.Pq, 74.50.+r, 74.62.En

Recently, the interplay of antiferromagnetic (AF) order and unconventional superconductivity in Ce-based heavy fermion superconductors CeMIn₅ (M = Co, Rh, Ir) have been intensively studied.^{1–13} For instance, CeCoIn₅ is a superconductor with the highest transition temperature $T_c \approx 2.3$ K, whereas CeRhIn₅ orders antiferromagnetically below $T_N \approx 3.7$ K.⁹ On the other hand, superconductivity is observed in the latter compound by application of pressure, whereas unconventional superconductivity in CeCoIn₅⁹ emerges in close proximity to an AF quantum critical point as in the cuprates and pnictides superconductors. Moreover, neutron scattering experiments indicate strong AF quasielastic excitations at wave vectors $Q = (\frac{1}{2}, \frac{1}{2}, \frac{1}{2})$ and equivalent positions in the paramagnetic regime. When entering the superconducting state, the magnetic excitations spectra by inelastic neutron scattering show the appearance of a sharp spin resonance.¹⁰ These findings underline the analogy to the cuprate high-temperature superconductors^{14,15} and the new iron superconductors,^{16,17} where AF spin fluctuations may actually mediate unconventional superconductivity.

So far, the superconducting pairing symmetry in CeCoIn₅ has been discussed from both experimental and theoretical sides, it has not yet been determined unambiguously. Soon after the discovery of CeCoIn₅ material, its Fermi surface (FS) has been studied in detail by quantum oscillation, which consists of a nearly cylindrical one and small ellipsoidal ones. The cylindrical sheets reflect quasi-two-dimensional (2D) character, by analogy with cuprates. Then the pairing state in CeCoIn₅ has been widely believed to be unconventional with d -wave symmetry with vertical line node. The early thermal conductivity and specific heat have been measured in a rotating magnetic field, and gave a controversial result on whether CeCoIn₅ has a superconducting gap with $d_{x^2-y^2}$ or d_{xy} pairing symmetry.^{18–21} The latter d_{xy} pairing symmetry was also inferred from the anisotropy in the high-field superconducting phase.²² Recent specific heat measurements²³ from the same group of Ref. 21 observed the predicted inversion of the oscillations²⁴ at lower temperature, which seemed to solve the dispute in favor of the $d_{x^2-y^2}$ case. In addition, detection of a magnetic resonance in neutron scattering experiment¹⁰ and Bogoliubov quasiparticle scattering interference imaging technique also suggest a $d_{x^2-y^2}$ pairing symmetry may be more favorable.²⁵ Theoretically, detailed calculations of the spin

resonance show that the resonance can appear only for the $d_{x^2-y^2}$ pairing symmetry but not in the d_{xy} case.²⁶ The recent field-angle-resolved anisotropy in the specific heat calculations also indicates the different features by considering the pairing gap functions $d_{x^2-y^2}$ and d_{xy} .²⁷

Although the ideally field-angle-resolved thermal conductivity and specific heat measurements can give the position of the nodes, they rely on the ability to accurately model the true electronic structure, which in fact is poorly understood in heavy fermion materials. It is also interesting to find that the universal limit of the residual term in the thermal conductivity is not obeyed with the La doped in CeCoIn₅,²⁸ where the contrasting behavior between thermal conductivity and specific heat with increasing impurities reveals the presence of uncondensed electrons coexisting with nodal quasiparticles. The recent muon knight shift measurements also found that the magnetic field dependence of the reduction of the muon knight shift is not in proportion to \sqrt{H} , which is roughly explained by the Fermi liquid relation and is inconsistent with the simple expectation for d -wave superconductors.²⁹ These facts likely reflect the multiband nature of superconductivity in CeCoIn₅, similar to the story of Fe-based superconductors.^{16,17}

On the other hand, de Hass–van Alphen (dHvA) experiments in CeCoIn₅ clearly indicate that the FS is three dimensional (3D).^{30–32} If quasi-2D FS (a large FS denoted as β band in the dHvA experiments) is strictly cylindrical along the k_z direction, the hot lines would be parallel to k_z . In this case, a neutron scattering resonance could be interpreted as a 2D spin excitation by analogy with cuprates as evidence of $d_{x^2-y^2}$ pairing symmetry with vertical line node, and should be observed for the whole set of momenta $Q = (\frac{1}{2}, \frac{1}{2}, x)$ with $0 \leq x \leq \frac{1}{2}$. However, this explanation of the resonance in CeCoIn₅ disagrees with the experiments where the neutron scattering resonance is only found at $Q = (\frac{1}{2}, \frac{1}{2}, \frac{1}{2})$.^{10,26} In Ref. 33 the authors argued that the absence of strong resonances at other momenta may be due to the fact that the quasi-2D FS was not perfectly cylindrical as evidenced by the existence of three different dHvA orbits that the gap parameter generally varied along the z axis, and that 3D FS should also have had contributions.³³ Thus they proposed a potential candidate—the “magnon” scenario for spin resonance in 3D superconductor in CeCoIn₅, which did not require a $d_{x^2-y^2}$ gap.

Since most of the experimental evidence for d -wave pairing symmetry is indirect, further theoretical and direct experimental work such as ARPES measurements and phase sensitive experiments are still needed and necessary to identify the order parameter in CeCoIn₅. In this paper we propose to use a local electronic structure around a single nonmagnetic impurity to probe the pairing symmetry in the CeCoIn₅ superconductor, since such properties have proved to be successful in identifying the unconventional pairing states of different classes of superconductors.^{34–40} Within a coherent 3D Anderson lattice model and the T -matrix approximation approach, we theoretically calculate the local density of states in the unitary limit of impurity scattering, and find that although both total density of states exhibit a similar V-shaped gaplike feature, the impurity induced intragap resonance state only occurs when the pairing symmetry is of $d_{x^2-y^2}$, similar to the case of the d -wave cuprate superconductor. Our prediction can be directly measured by scanning tunneling microscopy experiments in the heavy fermion superconductor CeCoIn₅.

According to band structure calculations,^{30–32,41,42} CeCoIn₅ comprises several f bands and conduction bands which are hybridized in a complex manner. Due to a large spin-orbit coupling the Ce- $4f$ electron states are split into upper $j = 7/2$ and lower $j = 5/2$ states, the latter one is further split into three crystalline electric field (CEF) Kramers doublet states. Because CEF splitting energy is much bigger than the heavy quasiparticle bandwidth (about 4 meV), we can restrict ourselves to the lowest CEF doublet which has an effective pseudospin 1/2. Thus here we consider a 3D coherent Anderson lattice model which could reproduce the result of band calculations, realize real FS, and is also technically manageable for a T -matrix calculation in the superconducting states. In fact, this has been done previously for CeCoIn₅,⁴³ and the resulting hybridized quasiparticle energy dispersion can be read as

$$E_{\mathbf{k}\pm} = \frac{1}{2}[(\varepsilon_{\mathbf{k}}^c + E_{\mathbf{k}}^f) \pm \sqrt{(E_{\mathbf{k}}^f - \varepsilon_{\mathbf{k}}^c)^2 + 4V_{\mathbf{k}}^2}], \quad (1)$$

where $\varepsilon_{\mathbf{k}}^c$ and $E_{\mathbf{k}}^f$ are the effective f band and the conduction band dispersions, respectively, and $V_{\mathbf{k}}$ is the effective hybridization strength, which is renormalized by the on-site f - f Coulomb repulsion. The detailed $\varepsilon_{\mathbf{k}}^c$, $E_{\mathbf{k}}^f$, and $V_{\mathbf{k}}$ as well as the parameters are defined as in Ref. 43, and the resulting FS is shown in Fig. 1. Note that band $E_{\mathbf{k}-}$ reproduces the above FS and is denoted as the β band in the de Hass–van Alphen experiments.^{30–32} While band $E_{\mathbf{k}+}$ remains above the Fermi energy, and thus has no contribution to the FS topological structure. Therefore, the novel low energy electronic state properties of CeCoIn₅ mainly originate from the band $E_{\mathbf{k}-}$.

In the superconducting state, the bare Green's function within the Nambu space is given by

$$\hat{G}_0^{-1}(\mathbf{k}, i\omega_n) = i\omega_n \hat{1} - \begin{pmatrix} E_{\mathbf{k}+} & \Delta_{\mathbf{k}} & 0 & 0 \\ \Delta_{\mathbf{k}} & -E_{\mathbf{k}+} & 0 & 0 \\ 0 & 0 & E_{\mathbf{k}-} & \Delta_{\mathbf{k}} \\ 0 & 0 & \Delta_{\mathbf{k}} & -E_{\mathbf{k}-} \end{pmatrix}, \quad (2)$$

where $\omega_n = (2n + 1)\pi T$ is the Matsubara frequency for fermions. The superconducting gap function is described by

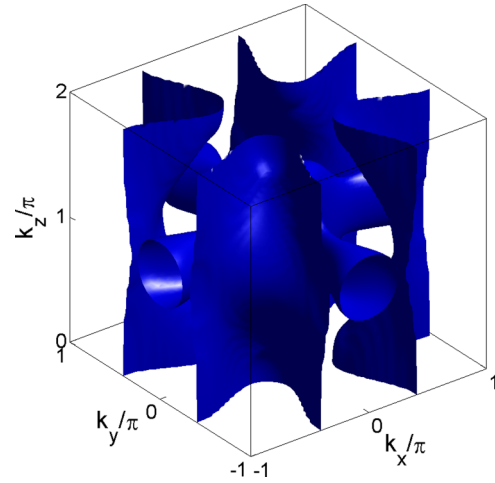


FIG. 1. (Color online) Calculated Fermi surface for CeCoIn₅ using the band structure parameters defined in Ref. 42.

$\Delta_{\mathbf{k}}$. Then the corresponding bare real-space Green's function can be obtained from the Fourier transform as

$$\hat{G}_0(i, j; i\omega_n) = \frac{1}{N} \sum_{\mathbf{k}} e^{i\mathbf{k}\cdot\mathbf{R}_{ij}} \hat{G}_0(\mathbf{k}, i\omega_n), \quad (3)$$

where $\mathbf{R}_{ij} = \mathbf{R}_i - \mathbf{R}_j$, with \mathbf{R}_i being the lattice vector and N is the number of lattice sites. In the presence of a single-site nonmagnetic impurity of strength U_0 located at the origin $r_i = 0$, the site dependent Green's function in term of the T -matrix approach can be obtained as

$$\hat{G}(i, j; i\omega_n) = \hat{G}_0(i, j; i\omega_n) + \hat{G}_0(i, 0; i\omega_n) \hat{T}(i\omega_n) \hat{G}_0(0, j; i\omega_n), \quad (4)$$

where

$$\hat{T}(i\omega_n) = \frac{\hat{U}_0}{\hat{1} - \hat{G}_0(0, 0; i\omega_n) \hat{U}_0} \quad (5)$$

and the potential scattering matrix takes the following structure:

$$\hat{U}_0 = \begin{pmatrix} U_0 & 0 & V & 0 \\ 0 & -U_0 & 0 & -V \\ V & 0 & U_0 & 0 \\ 0 & -V & 0 & -U_0 \end{pmatrix}, \quad (6)$$

where U_0 and V are the strength of the intra- and interband scattering potential.

The local density of states (LDOS) which is proportional to the local differential tunneling conductance measured by STM experiment can be expressed as

$$\rho(i, \omega) = -\frac{1}{\pi} \text{ImTr}[\hat{G}(i, i; i\omega_n \rightarrow \omega + i0^{\dagger})]. \quad (7)$$

The above scheme is sufficiently general to capture the essential properties of the single impurity scattering in a two-band superconductor. For the present case, the FS crossing originates only from band $E_{\mathbf{k}-}$ as discussed above, while band $E_{\mathbf{k}+}$ contributes little to the density of states (DOS) near Fermi energy. Therefore, it will be reasonable in the following calculations to only consider the impurity scattering effect in

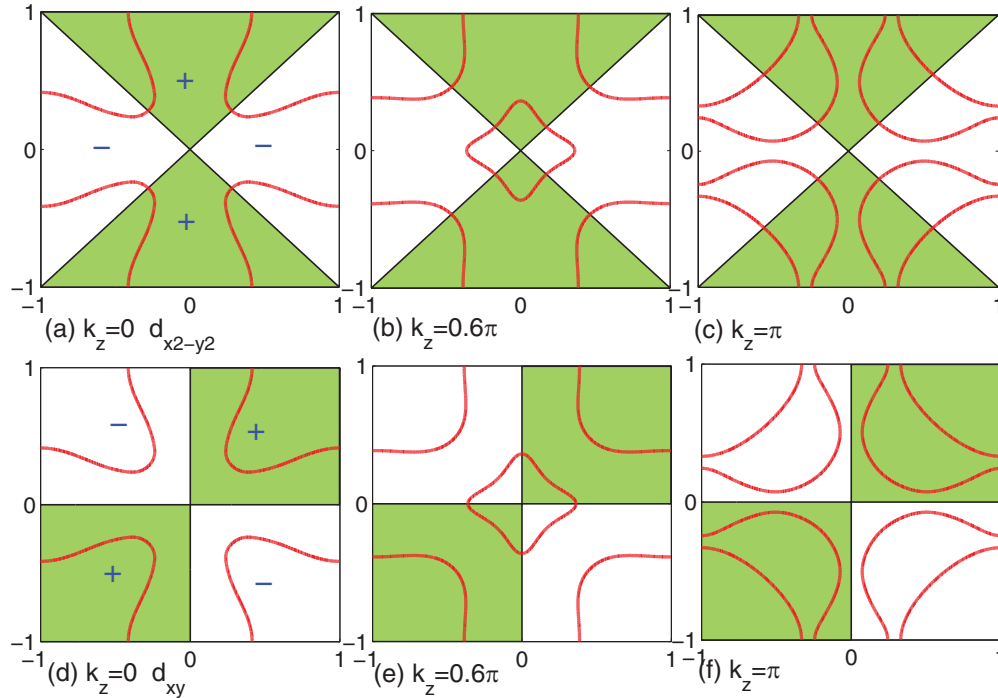


FIG. 2. (Color online) The Fermi surface topological structure and the pairing gap function in the first Brillouin zone for individual k_z . The upper panels indicate the pairing state with $\Delta_{\mathbf{k}} = \Delta_0(\cos k_x - \cos k_y)/2$ for (a) $k_z = 0$, (b) $k_z = 0.6\pi$, and (c) $k_z = \pi$, while the lower panels are for the case of d_{xy} gap symmetry with (d) $k_z = 0$, (e) $k_z = 0.6\pi$, and (f) $k_z = \pi$. The red solid lines denote the FS and the black lines indicate the node lines, \pm denotes the sign of the superconducting gap.

intraband $E_{\mathbf{k}-}$, and ignore the scattering from band $E_{\mathbf{k}+}$ and the interband impurity scattering (i.e., $V = 0$).

Before investigating the effect of the single impurity scattering, we need to first look into the properties of DOS. Notice that the corrugated FS of CeCoIn₅ is characterized by three dimensionality and is not perfectly cylindrical along the (0 0 1) line, following the method applied in Ref. 44 we first restrict ourselves to the ab plane by averaging over the momenta in the k_z direction, and analyze the DOS and local electronic structure induced by a nonmagnetic impurity for each slice of the FS at a particular k_z , and then by averaging over the individual DOS and LDOS of each k_z slice to obtain the final total DOS and LDOS along the (001) direction.

The considered pairing symmetry includes two possible candidates as discussed above, namely $d_{x^2-y^2}$ gap symmetry with

$$\Delta_{\mathbf{k}} = \Delta_0(\cos k_x - \cos k_y)/2 \quad (8)$$

and d_{xy} gap symmetry with

$$\Delta_{\mathbf{k}} = \Delta_0(\sin k_x \sin k_y). \quad (9)$$

The magnitude of the d -wave gap parameter Δ_0 should in principle be determined self-consistently, but for the sake of allowing for an analytic calculation, it is reasonable to assume its value is known. And also for the convenience of comparison, we assume the value Δ_0 is the same for a different k_z layer and for both two pairing symmetries.

We now turn to analyze the FS topological structure and the gap function in the first Brillouin zone for individual k_z as shown in Fig. 2. The upper panels of Fig. 2 represent the FS evolution with the $d_{x^2-y^2}$ gap function, where the node lines cut

the FS (red solid line) at any value of k_z . While in the lower panels, the properties of the nodal structure are completely *different*. For small values $k_z < 0.6\pi$ the gap function with d_{xy} symmetry has no node points on the FS, but changes sign across two neighboring FS arcs. With increasing k_z to about 0.6π value the inner FS appears and gives rise to the nodal structure as seen in Fig. 2(e). As k_z gradually increases and approaches π in Fig. 2(f), a new FS topological structure occurs, then the node line keeps away from the FS and the node points on the FS again disappear.

The effect of the nodal structure on the FS can be clearly reflected by the calculated DOS which is proportional to the differential tunneling conductance tested by the tunneling experiment. In Fig. 3 the DOS for the normal state (black solid line), superconducting state with $d_{x^2-y^2}$ (red dashed line), and d_{xy} (blue dotted line) gap symmetry are plotted for different cuts of the FS at $k_z = 0, 0.6\pi, \pi$. For the d_{xy} pairing symmetry, a V-shaped DOS only at $k_z = 0.6\pi$ as shown in Fig. 3(b) is exhibited reflecting the existence of nodal structure, while in other values of k_z the DOS is characterized by a U-shaped feature due to the nodeless gap structure and is very similar to the case of conventional s -wave superconductors. While for the $d_{x^2-y^2}$ case the DOS always behaves to be a V-shaped character at all values of k_z because of the sign change within each FS arc. We also find that the DOS in normal state at small values of k_z is rather small near the Fermi energy compared to the case of larger $k_z \subseteq [0.6\pi, \pi]$.

We now proceed to analyze the response of the local electronic structure to the single nonmagnetic impurity scattering in the superconducting state of CeCoIn₅. In Fig. 4 we plot the LDOS of quasiparticles on the impurity's nearest neighboring

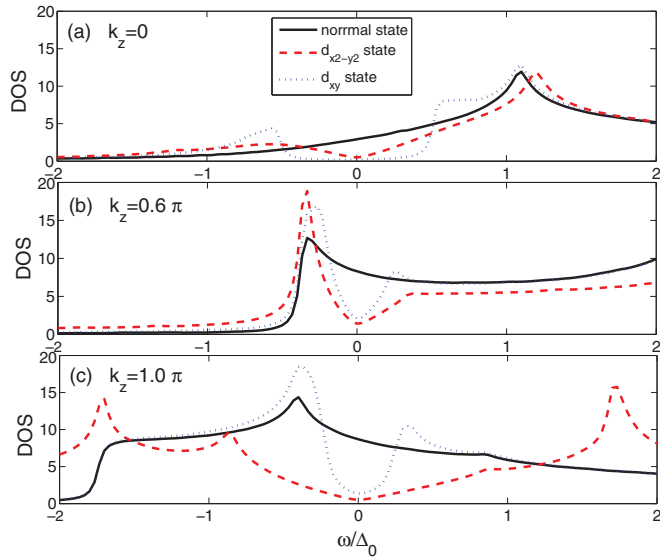


FIG. 3. (Color online) The DOS as a function of energy ω/Δ_0 for individual k_z with (a) $k_z = 0$, (b) $k_z = 0.6\pi$, and (c) $k_z = \pi$. The black solid line indicates the normal state, and the red dashed line and blue dotted line denote the superconducting states with $d_{x^2-y^2}$ and d_{xy} gap symmetry, respectively.

site for different FS cuts at $k_z = 0, 0.6\pi, \pi$ considering the impurity scattering strengthen in the unitary limit $U_0 = 100t$. The LDOS at $U_0 = 0$ (black solid line), which is equivalent to DOS in the clean system, shows two coherent peaks with different spectral weight due to the particle-hole asymmetry near the gap edges and other van Hove singularity peaks originated from the particular FS topological structure at different value of k_z .

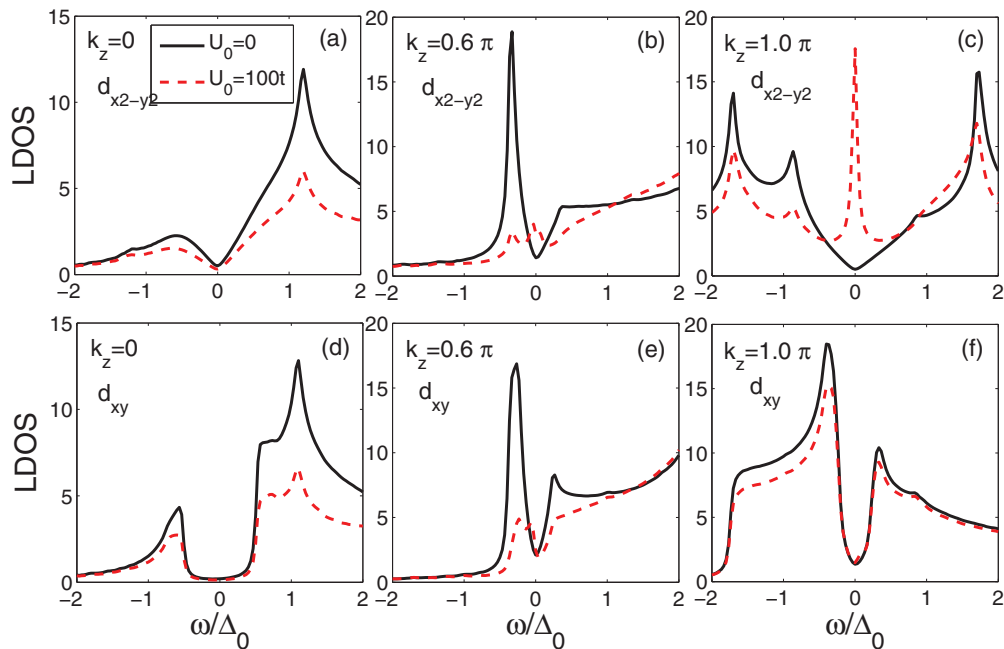


FIG. 4. (Color online) The LDOS spectra of quasiparticles on the impurity's nearest neighboring site for different scattering potentials U_0 . The upper panels indicate the pairing state with $\Delta_{\mathbf{k}} = \Delta_0(\cos k_x - \cos k_y)/2$ for (a) $k_z = 0$, (b) $k_z = 0.6\pi$, and (c) $k_z = \pi$, while the lower panels are for the case of d_{xy} gap symmetry with (d) $k_z = 0$, (e) $k_z = 0.6\pi$, and (f) $k_z = \pi$.

For the superconducting state with $d_{x^2-y^2}$ pairing symmetry as shown in the upper panels of Figs. 4(a)–4(c), we find that impurity induced resonance states near the Fermi energy occurs denoted by the resonance peaks (red dashed line), which is the result of the sign change within each FS arc due to the node line cutting the FS, and is similar to what happens in unconventional cuprate superconductors. At the same time, the superconducting coherent peaks are heavily suppressed. We also notice that the spectral weight of the resonance peak strongly depends on the special FS topological feature and therein the nodal structure. The impurity induced intragap resonance peak is almost invisible in Fig. 4(a), then is enhanced in Fig. 4(b), and finally is very sharp at the zero energy in Fig. 4(c). This is because the DOS contributions of the scattering electrons increase from $k_z = 0$ to $k_z = \pi$ due to the special nodal structure on the FS as shown in Figs. 2(a)–2(c), the spectral weight of the resonance peak is thus correspondingly enhanced. While for the d_{xy} pairing symmetry case we find that the impurity induced intragap resonance peak only occurs at $k_z = 0.6\pi$ as shown in Fig. 4(e), another value of k_z disappears and is replaced by resonance peaks near the gap edges. This is consistent with the aforementioned nodal structure and DOS.

Since the observable local electronic structure in CeCoIn₅ is of the three-dimensional (3D) feature and should be an average over the FS slices at different k_z , we have to consider the calculated DOS and LDOS averaged in the (001) direction. In this case we plot the averaged DOS and LDOS for the superconducting states with $d_{x^2-y^2}$ pairing symmetry and d_{xy} pairing symmetry in Fig. 5. We find that although both total DOS exhibit a similar V-shaped gaplike feature, only the $d_{x^2-y^2}$ -wave pairing symmetry gives rise to robust impurity resonance states reflected by a zero energy resonance peak in LDOS. Our result confirms the recent experimental results

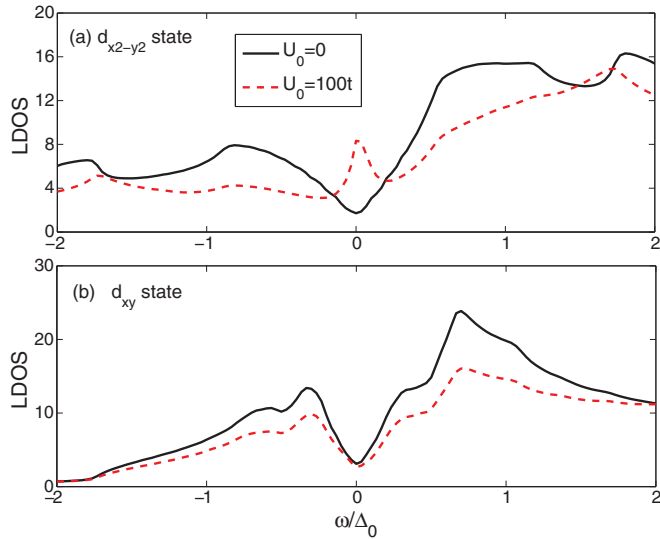


FIG. 5. (Color online) The calculated total LDOS spectra averaged in the (001) direction on the impurity's nearest neighboring site for different scattering potentials U_0 with (a) $d_{x^2-y^2}$ pairing state and (b) d_{xy} pairing state.

where such pairing breaking effect by impurities has been indirectly measured in CeCoIn₅ after doping a hole or electron.^{13,28} We propose that these features can be directly measured by scanning tunneling microscopy (STM) experiments, and then shed light on the pairing symmetry and pairing mechanism in CeCoIn₅ and other Ce-based heavy fermion superconductors, since they have the similar HoCoGa₅-type electronic structure.

In conclusion, by applying the T -matrix approximation approach we have studied the effect of a single

nonmagnetic impurity in CeCoIn₅ superconductor within a coherent Anderson lattice model which can reproduce the real 3D FS topological feature. We have found that, considering two types of pairing symmetry $d_{x^2-y^2}$ and d_{xy} , only $d_{x^2-y^2}$ pairing gives rise to a robust intragap impurity induced resonance state near the Fermi energy in the unitary limit of impurity scattering, though both pairing gaps in the superconducting state indicate the similar V-shaped feature of DOS. Based on these results, we propose to use STM experiment to test the local electronic structure around nonmagnetic impurities so as to identify the pairing symmetry and provide hints on the microscopic mechanism of unconventional superconductivity in the Ce-based heavy fermion superconductors.

After completing the present work, we were made aware of the recent high-resolution STM experiment on the CeCoIn₅ superconductor,⁴⁵ where due to the cleaving procedure which could cut the surface at different k_z points, the STM spectrum is available for a different k_z plane. After analyzing the k_z plane measured in above experiment and its FS topology, we find it is basically located in the $k_z \subseteq [0.6\pi, \pi]$ as shown in Figs. 2(b) and 2(c) and Figs. 2(e) and 2(f), and impurity-induced intragap bound states experimentally probed indeed confirm our theoretical predictions as seen in Figs. 4(b) and 4(c) for the $d_{x^2-y^2}$ pairing state.

We acknowledge helpful discussions with Professor Shiping Feng, Ilya Eremin, and Zhi Wang. This work was supported by the National Natural Science Foundation of China (NSFC) under Grant No. 11104011, Doctoral Fund of Ministry of Education of China under Grant No. 20110009120024, Research Funds of Beijing Jiaotong University under Grant No. 2013JBM092, and The Project sponsored by SRF for ROCS, SEM.

*liubin@bjtu.edu.cn

¹C. Petrovic, P. G. Pagliuso, M. F. Hundley, R. Movshovich, J. L. Sarrao, J. D. Thompson, Z. Fisk, and P. Monthoux, *J. Phys.: Condens. Matter* **13**, L337 (2001).

²H. Hegger, C. Petrovic, E. G. Moshopoulou, M. F. Hundley, J. L. Sarrao, Z. Fisk, and J. D. Thompson, *Phys. Rev. Lett.* **84**, 4986 (2000).

³R. A. Fisher, F. Bouquet, N. E. Phillips, M. F. Hundley, P. G. Pagliuso, J. L. Sarrao, Z. Fisk, and J. D. Thompson, *Phys. Rev. B* **65**, 224509 (2002).

⁴Y. Kawasaki, S. Kawasaki, M. Yashima, T. Mito, G.-q. Zheng, Y. Kitaoka, H. Shishido, R. Settai, Y. Haga, and Y. Onuki, *J. Phys. Soc. Jpn.* **72**, 2308 (2003).

⁵M. Yashima, S. Kawasaki, Y. Kawasaki, G.-q. Zheng, Y. Kitaoka, H. Shishido, R. Settai, Y. Haga, and Y. Onuki, *J. Phys. Soc. Jpn.* **73**, 2073 (2004).

⁶G.-q. Zheng, K. Tanabe, T. Mito, S. Kawasaki, Y. Kitaoka, D. Aoki, Y. Haga, and Y. Onuki, *Phys. Rev. Lett.* **86**, 4664 (2001).

⁷R. Movshovich, M. Jaime, J. D. Thompson, C. Petrovic, Z. Fisk, P. G. Pagliuso, and J. L. Sarrao, *Phys. Rev. Lett.* **86**, 5152 (2001).

⁸S. Kawasaki, G.-q. Zheng, H. Kan, Y. Kitaoka, H. Shishido, and Y. Onuki, *Phys. Rev. Lett.* **94**, 037007 (2005).

⁹J. L. Sarrao and J. D. Thompson, *J. Phys. Soc. Jpn.* **76**, 051013 (2007).

¹⁰C. Stock, C. Broholm, J. Hudis, H. J. Kang, and C. Petrovic, *Phys. Rev. Lett.* **100**, 087001 (2008).

¹¹M. Kenzelmann, Th. Strassel, C. Niedermayer, M. Sgrist, B. Padmanabhan, M. Zolliker, A. D. Bianchi, R. Movshovich, E. D. Bauer, J. L. Sarrao, and J. D. Thompson, *Science* **321**, 1652 (2008).

¹²S. Nair, O. Stockert, U. Witte, M. Nicklas, R. Schedler, K. Kiefer, J. D. Thompson, A. D. Bianchi, Z. Fisk, S. Wirth, and F. Steglich, *Proc. Natl. Acad. Sci. USA* **107**, 9537 (2010).

¹³K. Gofryk, F. Ronning, J.-X. Zhu, M. N. Ou, P. H. Tobash, S. S. Stoyko, X. Lu, A. Mar, T. Park, E. D. Bauer, J. D. Thompson, and Z. Fisk, *Phys. Rev. Lett.* **109**, 186402 (2012).

¹⁴Y. Sidis, *Phys. Status Solidi B* **241**, 1204 (2004).

¹⁵S. M. Hayden, H. A. Mook, P. Dai, T. G. Perring, and F. Dogan, *Nature (London)* **429**, 531 (2004).

¹⁶Chenglin Zhang, Meng Wang, Huiqian Luo, Miaoyin Wang, Mengshu Liu, Jun Zhao, D. L. Abernathy, T. A. Maier, Karol Marty, M. D. Lumsden, Songxue Chi, Sung Chang, Jose A. Rodriguez-Rivera, J. W. Lynn, Tao Xiang, Jiangping Hu, and Pengcheng Dai, *Sci. Rep.* **1**, 115 (2011).

¹⁷P. Dai, J. Hu, and E. Dagotto, *Nat. Phys.* **8**, 709 (2012).

¹⁸Y. Matsuda and K. Izawa, *Physica C* **388-389**, 487 (2003).

¹⁹Y. Matsuda and K. Izawa, *J. Low Temp. Phys.* **131**, 429 (2003).

²⁰K. Izawa, H. Yamaguchi, Y. Matsuda, H. Shishido, R. Settai, and Y. Onuki, *Phys. Rev. Lett.* **87**, 057002 (2001).

- ²¹H. Aoki, T. Sakakibara, H. Shishido, R. Settai, Y. Ōnuki, P. Miranovi, and K. Machida, *J. Phys.: Condens. Matter* **16**, L13 (2004).
- ²²R. Ikeda and H. Adachi, *Phys. Rev. B* **69**, 212506 (2004).
- ²³K. An, T. Sakakibara, R. Settai, Y. Onuki, M. Hiragi, M. Ichioka, and K. Machida, *Phys. Rev. Lett.* **104**, 037002 (2010).
- ²⁴A. B. Vorontsov and I. Vekhter, *Phys. Rev. B* **75**, 224501 (2007).
- ²⁵M. P. Allan, F. Massee, D. K. Morr, J. van Dyke, A. W. Rost, A. P. Mackenzie, C. Petrovic, and J. C. Davis, *Nat. Phys.* **9**, 468 (2013).
- ²⁶I. Eremin, G. Zwirnagl, P. Thalmeier, and P. Fulde, *Phys. Rev. Lett.* **101**, 187001 (2008).
- ²⁷T. Das, A. B. Vorontsov, I. Vekhter, and M. J. Graf, *Phys. Rev. B* **87**, 174514 (2013).
- ²⁸M. A. Tanatar, J. Paglione, S. Nakatsuji, D. G. Hawthorn, E. Boaknin, R. W. Hill, F. Ronning, M. Sutherland, L. Taillefer, C. Petrovic, P. C. Canfield, and Z. Fisk, *Phys. Rev. Lett.* **95**, 067002 (2005).
- ²⁹W. Higemoto, A. Koda, R. Kadono, K. Ohishi, Y. Haga, H. Shishido, R. Settai, and Y. Onuki, *J. Phys.: Conf. Ser.* **225**, 012013 (2010).
- ³⁰Y. Haga, Y. Inada, H. Harima, K. Oikawa, M. Murakawa, H. Nakawaki, Y. Tokiwa, D. Aoki, H. Shishido, S. Ikeda, N. Watanabe, and Y. Onuki, *Phys. Rev. B* **63**, 060503 (2001).
- ³¹Donavan Hall, E. C. Palm, T. P. Murphy, S. W. Tozer, C. Petrovic, Eliza Miller-Ricci, Lydia Peabody, Charis Quay Huei Li, U. Alver, R. G. Goodrich, J. L. Sarrao, P. G. Pagliuso, J. M. Wills, Z. Fisk, *Phys. Rev. B* **64**, 064506 (2001).
- ³²H. Shishido, T. Ueda, S. Hashimoto, T. Kubo, R. Settai, H. Harima, and Y. Onuki, *J. Phys.: Condens. Matter* **15**, L499 (2003).
- ³³A. V. Chubukov and L. P. Gor'kov, *Phys. Rev. Lett.* **101**, 147004 (2008).
- ³⁴A. V. Balatsky, I. Vekhter, and J.-X. Zhu, *Rev. Mod. Phys.* **78**, 373 (2006).
- ³⁵J.-X. Zhu, R. Yu, A. V. Balatsky, and Q. Si, *Phys. Rev. Lett.* **107**, 167002 (2011).
- ³⁶S. Onari and H. Kontani, *Phys. Rev. Lett.* **103**, 177001 (2009).
- ³⁷D. Zhang, *Phys. Rev. Lett.* **103**, 186402 (2009).
- ³⁸Y. Dubi and A. V. Balatsky, *Phys. Rev. Lett.* **104**, 166802 (2010).
- ³⁹B. Liu and I. Eremin, *Phys. Rev. B* **78**, 014518 (2008).
- ⁴⁰B. Liu and X. Hu, *Phys. Rev. B* **81**, 144504 (2010); *J. Phys. Chem. Solids* **72**, 380 (2011).
- ⁴¹T. Maehira, T. Hotta, K. Ueda, and A. Hasegawa, *J. Phys. Soc. Jpn.* **72**, 854 (2003).
- ⁴²Y. Onuki, R. Settai, K. Sugiyama, T. Takeuchi, T. Kobayashi, Y. Haga, and E. Yamamoto, *J. Phys. Soc. Jpn.* **73**, 769 (2004).
- ⁴³K. Tanaka, H. Ikeda, Y. Nisikawa, and K. Yamada, *J. Phys. Soc. Jpn.* **75**, 024713 (2006).
- ⁴⁴A. Akbari, P. Thalmeier, and I. Eremin, *Phys. Rev. B* **84**, 134505 (2011).
- ⁴⁵B. B. Zhou, S. Misra, E. H. da Silva Neto, P. Aynajian, R. E. Baumbach, J. D. Thompson, E. D. Bauer, and A. Yazdani, *Nat. Phys.* **9**, 474 (2013).